Appendix A

Recovery of Atmospheric Parameters From Radio Tracking Data of the Geodynamics Experiment

P. E. Schmid[a] *and S. Rangaswamy*[b]

INTRODUCTION

The primary goal of the Apollo-Soyuz Test Project (ASTP) Geodynamics Experiment (MA-128) was Earth gravity-field analysis. However, selected segments of MA-128 Doppler tracking data, as measured by the Applications Technology Satellite 6 (ATS-6), are also being studied in terms of lower atmosphere (i.e., tropospheric) effects. Certain results from this atmospheric analysis that have potential widespread application in the field of meteorology are presented in this appendix.

The biasing effects of the troposphere and the ionosphere on radio tracking data have been a subject of continuing study by the NASA Goddard Space Flight Center (refs. A-1 to A-3). This work has led to the development of algorithms that, to the extent possible, remove atmospheric effects from radio and laser tracking data. This research has been part of an NASA effort to improve satellite orbit determination accuracy.

The earlier applied atmospheric research indicated that Doppler tracking of a near-Earth satellite by means of a geostationary satellite near the time of occultation should provide a very pronounced range-rate signature of approximately tens of meters per second. Such a signature is well above the noise level that was observed to be approximately 0.03 cm/sec (ref. A-4) during the experiment. Analysis also indicated that such occultation data would provide a new means of deducing atmospheric pressure and temperature profiles on a worldwide basis. Such information would be invaluable to meteorologists involved in weather and climate research. The ASTP Geodynamics Experiment data provided the first opportunity to experimentally verify these concepts. The computational techniques and results associated with MA-128 occultation Doppler (range rate) analysis are presented in this appendix.

COMPUTATIONAL APPROACH

The radio occultation method of measuring planetary atmospheric parameters has been used to study the atmospheres of Mars and Venus (refs. A-5 and A-6). The technique consists of measuring the integral phase change of the tracking signal due to refraction by the atmosphere. During near-Earth occultation, the neutral atmosphere, or troposphere, will introduce the major refractive perturbation. The troposphere can be considered to extend from sea level to a height of approximately 30 km. The corresponding index of refraction varies from approximately 1.000350 at sea level to 1.000004 at the 30-km level. In terms of refractivity N, this variation corresponds to $4 < N < 350$. The ionosphere, which extends from approximately 85 to 1000 km, introduces a refractive effect that is inversely proportional to frequency squared (ref. A-3). Although the ionosphere is not a critical factor for near-Earth occultation, it certainly must be considered during any signature analysis at the centimeter per second level. There are now indications that the

[a]NASA Goddard Space Flight Center.

[b]Old Dominion Systems, Inc., Gaithersburg, Maryland.

"Himalayan data anomaly" observed near the end of several MA-128 passes is at least partly due to the steep ionospheric gradients characteristic of this region.

Planetary analysis involved transmission of radio signals from a spacecraft to Earth as the spacecraft passed into the planetary atmosphere just before occultation. In an analogous manner, Earth atmospheric radio occultation can be observed by means of a high satellite, such as the "geostationary" ATS-6, observing a near-Earth satellite in a satellite-to-satellite tracking configuration (refs. A-7 to A-10). During portions of MA-128, this was the desired configuration that provided the first useful data set for evaluating this concept. The "geostationary" ATS-6 satellite is actually in a slightly inclined equatorial orbit. Hence, the Doppler effect between ATS-6 and a ground station is not zero but varies sinusoidally with a period of 24 hours and a peak amplitude of a few meters per second (ref. A-11). The composite Doppler data recorded in this experiment are a result of the two satellite motions (ATS-6 and Apollo) and the coherent two-way Doppler equipment configuration. For the Apollo occultation analysis, the following approximation (ref. A-9) has proved adequate.

$$f_d = \left(2.256 \times 10^9\right)\left(-\frac{2}{c}\right)\left[\left(1 + \frac{1.7000}{2.256}\right)\dot{r}_1 + \dot{r}_2\right] \quad \text{(A1)}$$

where f_d is Doppler shift, the ATS-6 to Apollo carrier frequency is 2.256 GHz, c is the speed of light, 1.7000 is an exact multiplier resulting from the electronics, $\dot{r}_1$ is the average range rate from the Madrid station to ATS-6, and $\dot{r}_2$ is the average range rate from Apollo to ATS-6. It should be noted that the "raw data" consist of a measure of accumulated carrier phase change rather than carrier frequency change (ref. A-12). The carrier signal that originated at the Madrid site was transmitted to ATS-6 at 6 GHz, coherently relayed to and from Apollo at a nominal 2 GHz, and returned to Madrid at 4 GHz. The received signal at Madrid was processed in real time by the carrier Doppler extractor, and the data were recorded on standard punched paper tape. In the two-way 2-GHz link between ATS-6 and Apollo, each time the separation changed by one-half wavelength (≈7.5 cm), one cycle of Doppler phase was recorded. The path change between Madrid and ATS-6 also contributed to the overall Doppler phase measurement, although to a much lesser extent. That is, the Madrid to ATS-6 range rate was typically on the order of a few meters per second rather than the few kilometers per second associated with the ATS-6 to Apollo link. As shown by equation (A1), the Doppler frequency shift f_d is directly proportional to the average range rate. The data were recorded and time tagged as "nondestruct T-count" Doppler. In this mode, the accumulated phase change throughout a pass was recorded without clearing the counter while being read out at even time intervals. To obtain the desired resolution, the observed Doppler shift was electronically multiplied by a factor of 100 and offset with a fixed and stable 20-MHz bias signal. The net change in cycle count Δm over any time interval Δt is given by

$$\Delta m = \Delta t \left(f_b + 100 f_d\right) \quad \text{(A2)}$$

where f_b is a 20-MHz bias added to detect changes in range-rate sign and f_d is Doppler shift as defined in equation (A1).

As the near-Earth satellite (Apollo in this case) emerges from or enters radio shadow behind the Earth, the signal phase, and hence its time derivative or frequency, is abruptly affected by the presence of the atmosphere. The result is a large perturbation to f_d (eq. (A1)) of short duration (typically less than a minute). The computational approach was to determine accurately the orbits of ATS-6 and Apollo using all the available ground-tracking data obtained in support of ASTP. Then, $\dot{r}_1$ and $\dot{r}_2$ in equation (A1) were computed on the basis of this accurate ephemeris information. The computed data then were used to determine the expected behavior of the data as recorded at Madrid in the form of cycle counts (eq. (A2)). The sudden deviation from predicted behavior in the region of occultation was then attributed to the lower atmosphere. The mathematics for relating this Doppler change to an index of refraction profile of the troposphere (refs. A-13 and A-14)

had been determined before the Apollo launch as part of the Nimbus-6/ATS-6 Tracking and Data Relay Experiment (T&DRE). Although Nimbus-6 was launched on June 12, 1975, before the ASTP mission, the scheduled T&DRE checkout phase precluded occultation experiments until October 1975. Thus, the ATS-6/Apollo-Soyuz configuration provided the first opportunity to check out the foregoing concepts. The term refractivity N, as suggested previously, is simply a convenient means for representing the index of refraction n, where

$$n = 1 + N\left(10^{-6}\right) \tag{A3}$$

Initially, a model of atmospheric refractivity profile is assumed that, for this particular study, was an exponential of the form

$$N(h) = N_0 \exp(-kh) \tag{A4}$$

where $N(h)$ is the refractivity at an altitude h above sea level, N_0 is the refractivity at sea level, and k is the decay constant. Using some initial estimates of the parameters of this model, one-way range rate between ATS-6 and Apollo is computed for 30 data points at 1-second intervals up to the loss of signal. The computed range-rate values are compared with the observed values, which were derived from the four-way range sum rate by assuming symmetry between the upward and downward paths. The parameters of the model are then adjusted by iterative differential correction until least-squares convergence is reached. The estimated values of the parameters are used to compute the atmospheric refractivity profile.

The refractivity N of the atmosphere is a function of pressure, temperature, and humidity as given by

$$N = \frac{77.6}{T}\left(P + \frac{4810e}{T}\right) \tag{A5}$$

where P and e are the atmospheric total pressure and water-vapor pressure, respectively, in millibars and T is the temperature in Kelvin (ref. A-15). By assuming a water-vapor profile and by using the hydrostatic equation, it is possible to deduce values of pressure and temperature (ref. A-13). In this study, ASTP tracking data have been used to derive atmospheric refractivity as well as pressure and temperature profiles, which, for revolution 8, have been independently verified with radiosonde data. As indicated in table A-I, the Apollo-Soyuz tracking data base contains many passes for which the geometry was favorable for this type of occultation analysis. Revolution 8 was one of the first data sets that became available from the Geodynamics Experiment (MA-128) data base; therefore, data from this revolution were used for the initial analysis. However, subsequent data reductions indicate that revolution 8 is typical, and the same consistent results are being obtained from each revolution analyzed. Passes processed to date include revolutions 7, 8, 19, 20, 21, and 22.

Earlier simulations (ref. A-13) showed that the ionospheric effect on the Doppler rate was much smaller than the tropospheric effect and that the Chapman model was quite adequate for the inversion of occultation data. The critical frequency of 4 MHz was taken from vertical incidence data obtained from the meteorological station at Khabarovsk, U.S.S.R. (lat. 48.3° N, long. 135.1° E), which was the only ionosonde station in the general vicinity of the occultation site for which data were available.

RESULTS

Figure A-1 shows the time variation of the atmospheric bias $\Delta\dot{r}$ on the one-way range rate just before loss of signal between Apollo and ATS-6 during revolution 8. The range-rate atmospheric bias is defined as

$$\Delta\dot{r} = \bar{\dot{r}}_2 - \dot{r}_2 \tag{A6}$$

where $\bar{\dot{r}}_2$ is the observed one-way range rate between Apollo and ATS-6 and $\dot{r}_2$ is the true one-way range rate along the line of sight between the two spacecraft computed from the known orbits. The basic observation is the Doppler frequency indicated by equation (A1). The observed range

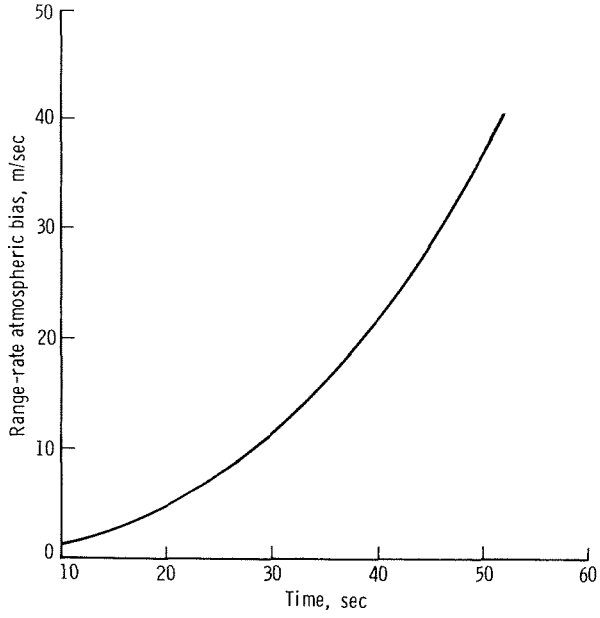

FIGURE A-1.—Time variation of atmospheric bias on the one-way range rate between Apollo and ATS-6. Data are from revolution 8, July 16, 1975, beginning at 07:48 UT. Loss of signal was at 53 seconds.

rate $\dot{\bar{r}}_2$ is obtained from equation (A1) by inserting the value of Doppler shift f_d obtained from the data (eq. (A2)) and by including the value of ATS-6 to Madrid site range rate $\dot{r}_1$, as computed using ATS-6 orbit information. The data used in this study to date were obtained during Apollo revolutions 7 and 8 on July 16, 1975. However, a careful survey of the total Doppler tracking data set indicates a large number of "highly probable" occultation passes at both the 1/second and 1/10-seconds data rates. These revolutions are indicated in table A-I. To the extent possible, these data will be used for further verification of the inversion technique presented in this report. The orbits of Apollo, as well as ATS-6, were determined by orbit computation using ground-tracking data. During the ASTP mission, ATS-6 was tracked by stations at Madrid, Spain, and Ahmadabad, India. The ATS-6 satellite was also tracked using the trilateration technique (ref. A-11) with transponders at Madrid, Ascension Island, and Johannesburg, South Africa. The Apollo spacecraft was tracked by the NASA Spaceflight Tracking and Data Network. Occultation during revolution 8 occurred at latitude 48.5° N, longitude 112.7° E. Radiosonde data from the meteorological station at Choybalsan, Mongolian Peoples Republic (lat. 48.0° N, long. 114.5° E) were used for comparison with revolution 8 results. Data for comparison with revolution 7 results have not yet been obtained. Table A-II gives the values of refractivity obtained from occultation data for revolution 8, as well as those derived from radiosonde data from the nearby meteorological station. In the case of

TABLE A-I.—Apollo Revolutions for Which Occultation Data Are Highly Probable

(a) For 1/second data rate

Revolution no.	*Date*	*Stop time, UT, hr:min*
6	July 16, 1975	04:38
7		06:15
8		07:49
17		21:54
19	July 17, 1975	00:59
20		02:35
21		04:12
22		05:49
23		07:23
82	July 21, 1975	04:33
83		06:07
84		07:40
85		09:12
87		12:22

(b) For 1/10-seconds data rate

Revolution no.	*Date*	*Stop time, UT, hr:min*
5	July 16, 1975	03:01
16		20:24
24	July 17, 1975	08:55
34	July 18, 1975	00:37
35		02:14
37		05:29
45		18:07
46		19:41
52	July 19, 1975	04:15
53		06:45
54		08:26
60		17:50
67	July 20, 1975	04:52
68		06:29
69		07:59
76		19:17
89	July 21, 1975	15:08
98	July 22, 1975	05:48

radiosonde data, the measured temperature, humidity, and pressure are sufficient to compute the reference refractivity profile. The radiosonde data were available only for 00:00 and 12:00 UT. Because the time of occultation was 07:49 UT, the radiosonde data corresponding to the occultation time were obtained by linear interpolation between the 00:00 and 12:00 UT data sets. Although this procedure may not have theoretical justification, the paucity of available data made it a practical necessity. It may be observed from table A-II that the difference between the two sets of refractivity at the 85 000-Pa (850 mbar) level is only 2.2 percent. It is conceivable that even better agreement between profiles would have been achieved had radiosonde data been available at the precise time of occultation. The two profiles provide the same value of refractivity at a height of approximately 6 km.

The occultation-derived refractivity profile was inverted to obtain the pressure profile by using an assumed average water-vapor profile. The technique used is presented in detail in reference A-13. After the pressure profile was obtained, the temperature profile was deduced from it by using equation (A5) and the radiosonde data for water-vapor pressure. The results, shown in table A-III, indicate that the agreement between the radiosonde- and occultation-derived pressure values at the 85 000-Pa (850 mbar) level is a difference of less than 1 percent, thus approaching the accuracy required for meteorological applications. A semilogarithmic plot comparing the two refractivity profiles is given in figure A-2. The Doppler-determined values of refractivity for Apollo revolution 7 occultation are presented in table A-IV.

TABLE A-II.—Results From Apollo and ATS-6 Atmospheric Parameters
[*Revolution 8, July 16, 1975*]

Altitude, km	*Pressure, Pa (mbar)*	*Refractivity*		*Difference, percent*
		Occultation derived	*Radiosonde derived*	
1.407	85 000 (850)	261.44	255.79	2.2
3.016	70 000 (700)	212.36	203.25	4.5
5.650	50 000 (500)	151.09	152.27	.8
7.280	40 000 (400)	122.39	128.75	−4.9
9.260	30 000 (300)	94.75	102.68	−7.7

TABLE A-III.—Atmospheric Data From Apollo/ATS-6 Occultation Data
[*Revolution 8, July 16, 1975*]

Altitude, km	*Pressure, Pa (mbar)*		*Difference, percent*	*Temperature, K*		*Difference, percent*
	Radiosonde derived	*Occultation derived*		*Radiosonde derived*	*Occultation derived*	
1.407	85 000 (850)	85 230 (852.3)	0.3	289.6	279.6	3.5
3.016	70 000 (700)	70 600 (706.0)	.9	276.8	268.6	2.9
5.650	50 000 (500)	50 900 (509.0)	1.8	256.5	263.6	2.8
7.280	40 000 (400)	41 350 (413.5)	3.4	242.3	263.0	8.5
9.260	30 000 (300)	32 060 (320.6)	6.9	227.1	262.8	15.7

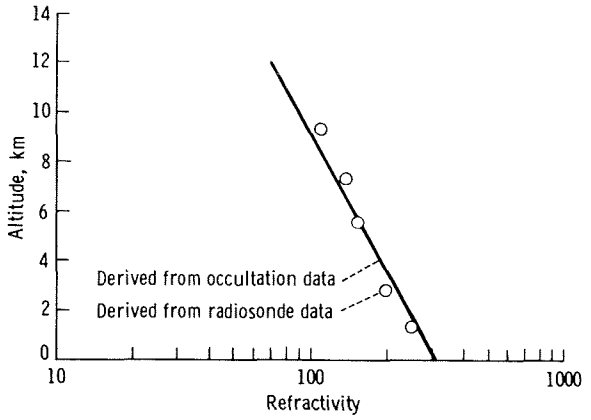

FIGURE A-2.—Refractivity profile from occultation data between Apollo and ATS-6. Data are from revolution 8, July 16, 1975, beginning at 07:48 UT.

TABLE A-IV.—Doppler-Determined Atmospheric Refractivity Profile
[*Revolution 7, July 16, 1975*]

Altitude, km	*Occultation-derived refractivity*
1	281.8
2	250.3
3	222.2
4	197.4
5	175.3
6	155.6
7	138.2
8	122.7
9	109.0
10	96.8

CONCLUSIONS

The analyses performed thus far clearly demonstrate the feasibility of using occultation between a near-Earth and a synchronous satellite to deduce atmospheric pressure and temperature profiles. The agreement of the occultation- and radiosonde-derived pressures and temperatures at the 85 000- and 70 000-Pa (850 and 700 mbar) levels is quite good considering that the radiosonde-derived reference profile was not exactly coincident in time and location with the occultation-derived profile. Data from Apollo revolutions 19, 20, 21, and 22 have been processed for occultation analysis. The profile extracted from revolution 22 data is very similar to that obtained from revolution 7 data. This similarity is not surprising because the occultation site (i.e., geographical latitude and longitude where the radio path just grazes the Earth) was the same for these two particular revolutions.

The possibility of using radio occultation of signals between two Earth-orbiting satellites to measure meteorological parameters for purposes of weather forecasting was recognized at least as early as 1969 (ref. A-16). These earlier ideas were adapted and refined (refs. A-13 and A-14) for application to the particular case of a geostationary satellite tracking a near-Earth satellite. The MA-128 experiment provided the very first data base to verify these theoretical considerations.

In long-term (i.e., greater than 10 days) weather forecasting, an accurate worldwide initial state of the atmosphere in terms of pressure, temperature, and humidity is essential. At present, such information is obtained from a variety of sources. These sources include balloonborne radiosonde, satellite radiometry, surface observations, and so forth. All such sources require a substantial cost in deploying specialized equipment and in establishing the logistics for worldwide data collection, integration, and distribution. The importance of the occultation scheme, which was demonstrated in this experiment, is that no special instrumentation is required, and worldwide coverage is inherent in the tracking geometry. Therefore, with any near-Earth satellite (such as will be tracked by the forthcoming NASA geostationary Tracking and Data Relay Satellite System (TDRSS)), the tracking data required for operational orbit computation can also be used to extract atmospheric parameters. Such parameters could then be used as a primary input for long-term weather forecasting with no additional expense or complexity beyond that always incurred from routine central facility computer processing together with subsequent distribution to the user community.

REFERENCES

A-1. Marini, J. W.: Correction of Satellite Tracking Data for an Arbitrary Tropospheric Profile. Radioscience, vol. 7, Feb. 1972, pp. 223-231.

A-2. Marini, J. W.: Tropospheric Range-Rate Tracking Data Correction. NASA TM X-66071, 1972.

A-3. Schmid, P. E.; Bent, R. B.; et al.: NASA-GSFC Ionospheric Corrections to Satellite Tracking Data. NASA TM X-70608, 1973.

A-4. Vonbun, F. O.; Kahn, W. D.; et al.: Geodynamics Experiment MA-128. Sec. 12 of Apollo-Soyuz Test Project Preliminary Science Report, NASA TM X-58173, 1976.

A-5. Fjeldbo, G.; Kliore, A.; and Eshleman, V. R.: The Neutral Atmosphere of Venus as Studied With the Mariner V Radio Occultation Experiments. Astron. J., vol. 76, 1971, pp. 123-140.

A-6. Fjeldbo, G.; and Eshleman, V. R.: The Atmosphere of Mars Analyzed by Integral Inversion of the Mariner IV Occultation Data. Planetary and Space Science, vol. 16, 1968, pp. 1035-1059.

A-7. Vonbun, F. O.; and Mengel, J. T.: Tracking and Communications for Planetary Manned Mission. J. Spacecraft & Rockets, vol. 5, no. 7, July 1968, pp. 863-865.

A-8. Vonbun, F. O.: The ATS-F/Nimbus-E Tracking Experiment. Rotation of the Earth, Paul Melchior and Shigeru Yumi, eds., D. Reidel Publ. Co. (Dordrecht, Holland), 1972, pp. 112-120.

A-9. Schmid, P. E.; and Vonbun, F. O.: The ATS-F/Nimbus-E Tracking and Orbit Determination Experiment. 1974 IEEE Intercon. Technical Program Papers, 1974, pp. 34/6-1 to 34/6-8.

A-10. Schmid, P. E.; Trudell, B. J.; and Vonbun, F. O.: ATS-6 Satellite-to-Satellite Tracking and Data Relay Experiments. IEEE Trans. Aerosp. and Electron. Sys., vol. AES-11, no. 6, Nov. 1975, pp. 1048-1058.

A-11. Schmid, P. E.; and Lynn, J. J.: Results of the 3 November 1974 Applications Technology Satellite-6 (ATS-6) Trilateration Test. NASA TM X-70897, 1975.

A-12. Bryan, J. W.; Lynn, J. J.; and Hinely, A. O.: A User's Guide for Satellite to Satellite System Observations and Data Formats. NASA TM X-70895, 1975.

A-13. Murray, C. W., Jr.; and Rangaswamy, R.: Recovery of Atmospheric Refractivity Profiles From Simulated Satellite-to-Satellite Tracking Data. NASA TM X-71016, 1975.

A-14. Rangaswamy, S.: Recovery of Atmospheric Parameters From the Apollo-Soyuz/ATS-F Radio Occultation Data. AGU Geophysical Research Letters, vol. 8, Aug. 1976, pp. 483-486.

A-15. Bean, B. R.; and Dutton, E. J.: Radio Meteorology. National Bureau of Standards, Monograph 92, Mar. 1966, p. 7.

A-16. Lusignan, Bruce; Modrell, Gary; et al.: Sensing the Earth's Atmosphere With Occultation Satellites. Proceedings of IEEE, vol. 57, no. 4, Apr. 1969, pp. 458-467.